Available online at www.sciencedirect.com
SCIENCE DIRECT®
International Journal of Mass Spectrometry 233 (2004) 117–123
International Journal of Mass Spectrometry
www.elsevier.com/locate/ijms

Signature of cluster isomers in time-resolved photodissociation experiments

M. Vogel [a,*], K. Hansen [b], L. Schweikhard [c]

[a] *Institut für Physik, Johannes-Gutenberg-Universität, D-55099 Mainz, Germany*
[b] *Chalmers University of Technology, Gothenburg University, SE-41296 Gothenburg, Sweden*
[c] *Institut für Physik, Ernst-Moritz-Arndt-Universität, D-17487 Greifswald, Germany*

Received 30 September 2003; accepted 16 December 2003

Abstract

The unrecognized presence of structure isomers in mass-selected cluster ensembles may obstruct investigations of the systems' intrinsic properties, since isomers differ not only in geometry, but also in other important properties. By the same token isomers are very interesting objects in the detailed study of atomic clusters. In the present work, different scenarios of isomeric coexistence are presented. They vary in the relative values of the interconversion barrier and the dissociation energies. For some idealized cases the possibility of a distinction of isomers by photodissociation experiments is discussed. In favorable situations isomeric structures may even be selected.

Keywords: Fragmentation; Nanoparticles; Charged clusters; Isomers

1. Introduction

Structure isomers of metal clusters have recently attracted increased interest. Numerous publications are concerned with both theoretical and experimental methods that allow to discern different isomeric structures and to acquire knowledge about their geometric properties [1–28]. Part of this interest arises from the fact that mass-selected ensembles of clusters may contain isomeric structures which differ in geometry and in other important aspects, as, e.g. dissociation energies and ionization potentials. A priori knowledge about the presence of isomers in a given experiment is in general unavailable and a mixture of isomeric structures may therefore obscure the interpretation of measurements of these quantities. The experimental results depend on the composition of the ensemble in the sense that some average of the different isomeric structures' properties will be measured.

In several special cases, fullerene or cluster ion production and subsequent separation of selected isomers has been experimentally achieved [19–22]. However, there are, to our knowledge, no cluster sources or general formation processes available that can produce defined geometric or electronic structures for free clusters. It is therefore highly desirable to be able to experimentally unveil and potentially control the presence of isomers.

The link between cluster geometry, stability and other properties of clusters has been studied intensively by theory [1–6,10–18]. For small clusters at low temperature in general various geometric structures exist which differ in dissociation energies [4–6,10,12–15,18]. For larger clusters, different regular geometrical packings as well as different amorphous ground state structures have been found theoretically [13–15,28], as well as structures with short range order [7–9]. In general the number of isomers grows very rapidly with cluster size. It also depends strongly on the range of the potential; long range potentials tend to give fewer isomers than those of short range [7]. The presence of both regular and amorphous structures may depend not only on the temperature, but also on details of the cluster formation process [14]. Especially for small systems, several stable isomers can be present even at room temperature [4–6,10,16–18].

Ion mobility measurements allow a reconstruction of the clusters' geometric properties by use of considerations that relate the cluster structure to the ion mobility in gases. They have been successfully applied, e.g. to the determination of gold and silver cluster geometries [23,25–27]. Elec-

* Corresponding author. Tel.: +49-06131-39-22891; fax: +49-06131-39-25169.
E-mail address: manuel.vogel@uni-mainz.de (M. Vogel).

1387-3806/$ – see front matter © 2004 Published by Elsevier B.V.
doi:10.1016/j.ijms.2003.12.027

tron diffraction measurements also allow a reconstruction of the cluster's geometric properties, as has been shown for *CsI*-clusters [29]. As a common feature of these investigations the geometry is probed indirectly by comparison of the experimental data with the predictions of modeling and simulations. Photoexcitation studies have the potential to yield complementary information on the isomers characteristic energies. In the following, a systematics of the potential cases and the possibility of an experimental distinction of cluster isomers in photodissociation experiments is discussed.

2. General considerations

In photodissociation experiments with size-selected clusters at low laser intensities, a unimolecular dissociation reaction of the kind

$$M_n^{\pm} \rightarrow M_m^{\pm} + M_{n-m} \quad (1)$$

is initiated by an excitation energy E if it exceeds the dissociation energy D_n of the system.

E is given as the sum of the thermal energy E_{th} of the cluster before photoexcitation and the photoexcitation energy E_γ. If the excitation energy E exceeds the dissociation energy D_n moderately, the dissociation occurs delayed on an observable timescale and can very often be described by unimolecular decay rate theory [30–34]. The delayed dissociation can be monitored in time-resolved photodissociation measurements (TRPD) [35,36]. Such experiments have been performed for several metal clusters [37–41] and rates of evaporation have been determined as a function of excitation energy. Probably the most extensive TRPD measurements have been made on cationic gold clusters stored in a Penning trap [38,39,42–44]. For most elements, unimolecular dissociation of cluster ions occurs by evaporation of a neutral monomer ($n - m = 1$). For monovalent metal cluster ions, neutral dimer evaporation ($n - m = 2$) is known to compete with monomer evaporation [45–50]. The two decay channels are not explicitly distinguished in this contribution. In fact, one isomer may decay exclusively via monomer evaporation while the other emits dimers without further implications for the arguments presented (see the subsequent text).

In the following, the discussion is restricted to the simple case of the presence of two isomeric structures I and II which are separated by a barrier of height ΔB, as measured from the minimum of the less stable isomer II to the top of the barrier. A schematic illustration is given in Figs. 1 and 2. The values of the dissociation energies D_I and D_{II} refer to the energy difference between the respective potential minimum and the lowest asymptotically free state the respective isomer has unhindered access to. For simplicity, we assume that there is no barrier for the inverse reaction. Isomer II is defined to be the less stable isomer, i.e. $D_{II} < D_I$. Note that isomer I does not necessarily represent the energetic ground state. The difference in dissociation energies $D_I - D_{II}$ is denoted by ΔD.

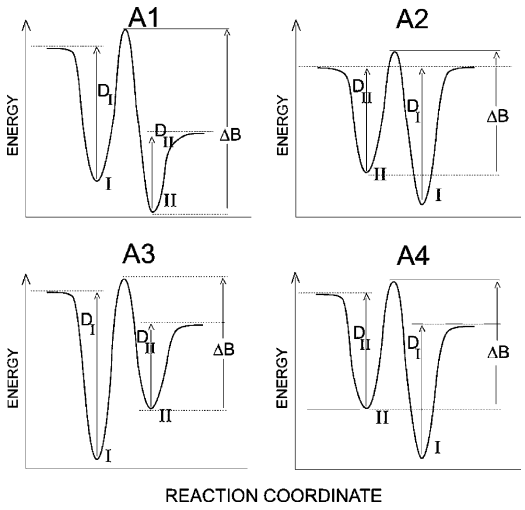

Fig. 1. Schematic representation of possible potential energy surfaces for a cluster with two isomers separated by a barrier exceeding both free fragment states.

Fig. 1 shows the possible cases where the isomers are separated by a barrier the top of which exceeds both asymptotically free states. In these cases and for moderate excitation energies the decay of one isomer is not influenced by the existence of the other isomer. Fig. 2 shows the possible cases where the isomers are separated by a barrier the top of which does not exceed both asymptotically free states. This means that upon excitation of the cluster, the decay of one isomer is influenced by the existence of the other. In the cases labeled "B" the top of the barrier lies

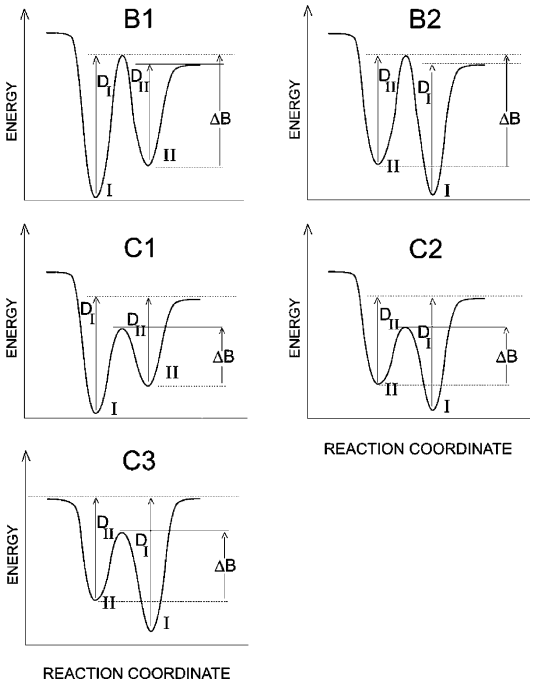

Fig. 2. Schematic representation of possible potential energy surfaces for a cluster with two isomers separated by a barrier which allows a mixing of states.

energetically between the asymptotically free states. In the cases labeled "C" it is below both. The case C3 is a special case with energetically identical free states, similar to case A2. Although it may seem that this degeneracy of the final state requires an accidental degeneracy of the two products, it is included explicitly in the list because the product states may be identical, even if the initial state is well represented by two distinct isomers. In fact, this situation will arise with certainty when the cluster is small enough.

The following analysis will be restricted to the cases shown in Fig. 1. The restriction is due to the difference in nature of the barrier crossing and the evaporation of an atom (or dimer). Different frequency factors $(8\pi g\mu/h^3)\sigma_{n-1}T^2$ in Eq. (2) (see Section 3) must be considered for these two different types of activated processes which makes the precise distinction between situations A and B, C a somewhat subtle task. Implicit in this restriction to cases A is therefore also an acknowledgment that the value of ΔB should be as high as needed to prevent crossing from one isomeric minimum to the other, and that this height may be more or less than the value sketched in the figure, depending on whether the frequency factors mentioned above are similar to each other or not. Another difficulty arises in the analysis of the cases B1 and, in particular, B2. It is not obvious whether a thermal excitation out of the minimum I (for B1) or II (for B2) will automatically lead to evaporation on a short timescale, or if the cluster will become trapped and thermalized in the other potential minimum. The quantitative analysis presented here is therefore restricted to cases of type A. It is not to be inferred that the remaining cases will not be susceptible to a similar analysis and experimental technique, but only that quantitative predictions require further knowledge of the systems.

3. Isomer decay rate constants

Upon excitation, a cluster undergoes a statistical unimolecular decay. In the case of neutral monomer evaporation and in the framework of detailed balance theory the decay rate is given by [34]:

$$k(E,n) = \frac{8\pi g\mu}{h^3}\sigma_{n-1}T^2\frac{\rho_{n-1}(E-D)}{\rho_n(E)} \quad (2)$$

where g is the degeneracy of the outgoing fragment channel, μ is its reduced mass, σ is the cross section for the inverse reaction and T is the microcanonical cluster temperature after evaporation. $\rho_{n-1}(E-D)$ is the level density of the product cluster, i.e. after evaporation of a neutral monomer, and $\rho_n(E)$ is the level density of the initial cluster before evaporation. The indices $n-1$ and n refer to the respective number of constituting atoms in the cluster.

Eq. (2) is derived from detailed balance which also allows to derive the rate constant for dimer evaporation. The main changes are that the reduced mass is changed by approximately a factor of two, that a factor corresponding to the rotational partition function of the dimer appears and that the product level density changes to that of the cluster two atoms smaller [34]. These changes are tractable and can be parametrized in a change of the frequency factor of the rate constant. As mentioned above for simplicity only monomer evaporation from both channels will be considered.

If only one isomer (i.e. one dissociation energy) is present, an ensemble of A_n clusters of size n excited by the same energy E shows an exponential decay of the kind

$$A_n(t) = A_n(0)\exp(-kt) \quad (3)$$

where $A_n(t)$ is the number of initial clusters remaining after time t following excitation and k is the decay rate constant given by (2). Consequently, the number of product clusters as a function of time is given by $A_{n-1}(t) = A_n(0) - A_n(t)$.

When two isomers are present, the decay rate constants will in general be different. Assuming rate constants k_{I} and k_{II}, the decay of the initial ensemble of size n clusters can be described by

$$A_n(t) = A_n^{\mathrm{I}}(0)\exp(-k_{\mathrm{I}}t) + A_n^{\mathrm{II}}(0)\exp(-k_{\mathrm{II}}t) \quad (4)$$

where the superscripts I and II refer to the isomers I and II.

The simple exponential form requires that all cluster in the ensemble have the same value of the internal excitation energy. In the extreme opposite case of a broad energy distribution the observed decay can be described by a power law in time [51]. But as discussed below, even for finite energy distributions it is possible to distinguish the isomeric decay components if the width of the distributions is sufficiently small.

When the excitation energy E is chosen above both D_{I} and D_{II}, both isomers will decay along the lowest energetically accessible trajectories at their respective rate constants. The strongest variation of the rate constants is caused by the dependence on E and D. In the following the implications on the experimental observation of the decay are discussed by way of specific examples. We note in passing that the situation of distinct precursor isomers described in this contribution is quite different from the decay from one well-defined state of the precursor a to two (or more) different products b and c, e.g. two different isomeric states or two different sizes. In this latter case one observes a simple exponential decay with a single rate constant k. However, there may be a second observable, namely the branching ratio for the decay products, if they can be distinguished experimentally (e.g. by mass spectrometry if the decay involves different cluster sizes). In this case partial decay rates k_b, k_c can be associated with the products such that their sum is equal to the observed decay rate, $k_b + k_c = k$, and that their ratio is the inverse of the observed product abundances: $k_b/k_c = A_b/A_c$ [42,50].

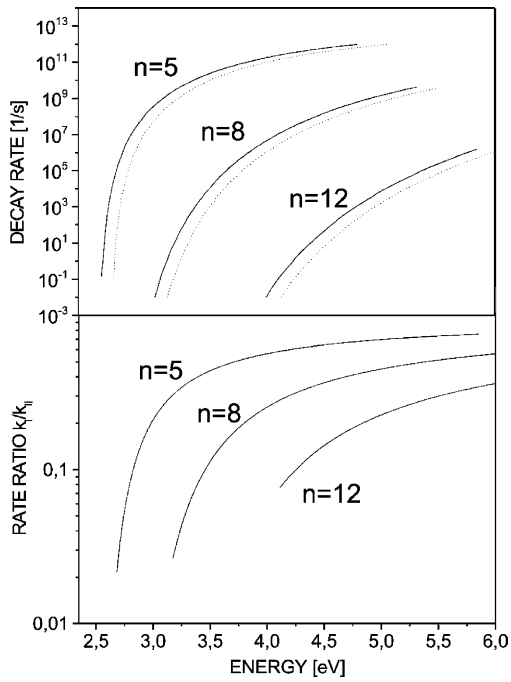

Fig. 3. Top: rates of fragmentation according to Eq. (2) as a function of the excitation energy for gold clusters Au_5^+, Au_8^+ and Au_{12}^+ (solid lines) when dissociation energies of 2.42, 2.65 and 2.91 eV are assumed. Dotted lines give the corresponding rates of fragmentation if the dissociation energy of the clusters were higher by 0.1 eV. For the calculation according to Eq. (2) the scaled bulk heat capacities [53] have been used in the parametrization given in [54] with parameters $a = -0.0093$ eV, $b = 3.821$ and $c = 11.009\,\text{eV}^{-1}$. The cross section σ has been assumed geometric, i.e. $\sigma(n) = \pi n^{2/3} r_S^2$ where r_S is the Wigner–Seitz radius of the neutral atom (1.59 Å). Bottom: ratio of decay rates k_I and k_{II} as shown in the top figure as a function of the excitation energy.

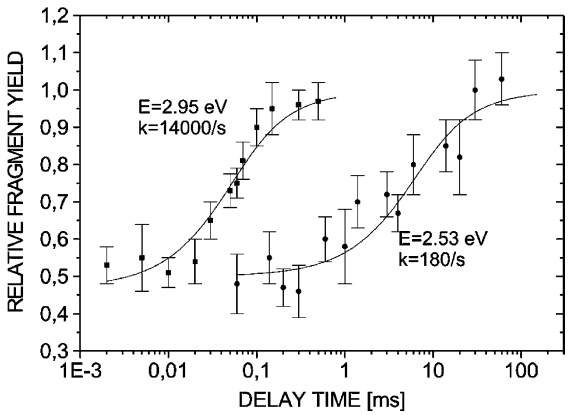

Fig. 4. Relative product cluster intensity as a function of delay time for the time-resolved decay of Au_{10}^+ at two different excitation energies of 2.53 and 2.95 eV, respectively.

4. Numerical examples

4.1. Rate differences

The upper part of Fig. 3 shows the rates of fragmentation as a function of excitation energy E according to Eq. (2) for gold cluster cations of sizes $n = 5$, $n = 8$ and $n = 12$ (solid lines). The choice of these clusters as examples is in principle arbitrary, however, gold clusters have been studied extensively by TRPD [35–39,42] and the cluster size region can be assumed relevant and accessible for the presented ideas (see the subsequent text).

For Au_5^+, Au_8^+ and Au_{12}^+ respective dissociation energies of 2.42, 2.65 and 2.91 eV have been used. Since the exact numbers of these values are not important for the current studies, the value for Au_{12}^+ has been deduced from TRPD data [52] by use of Eq. (2), the value for Au_8^+ results from a model-independent measurement [44] and the value for Au_5^+ is extrapolated [52] from model-independent dissociation energies as measured for Au_n^+, $n = 8$,14–24 [44]. In order to simulate the existence of a second isomeric state, dissociation rates of the same clusters are also shown (dotted lines) for dissociation energies that are 0.1 eV higher than the values given above.

In the lower part of Fig. 3, the ratio k_I/k_{II} as a function of the excitation energy is shown. The deviation of the ratio from unity (and thus the potential for an experimental revelation of the presence of isomers) is highest for an excitation energy slightly above the dissociation energy of the more stable isomer. On the other hand, the excitation energy needs to excess the dissociation energy sufficiently to produce a rate high enough for experimental observation of the decay. Thus, the experimental ability to uncover the presence of two different decay rates of a mass-selected ensemble depends strongly on the possible time range of the experiment and on the statistical significance of the data. Ion trap experiments may be best suited for this purpose since their possible time range spans values well above four orders of magnitude apart [55]. The size of the system influences strongly the necessary excitation energy to induce a decay at a rate high enough for experimental observation. These minimum rates may reach down to the order of $1\,\text{s}^{-1}$ in ion trap experiments, but in general, much higher rates will be needed for experimental observation of the decay. In the present context, the behavior shown in Fig. 3 can be considered representative at least for group-11-metal clusters and qualitatively also for most transition metal clusters.

Fig. 4 shows experimental data on the TRPD of Au_{10}^+ measured in a Penning trap: the relative product cluster intensity (normalized to the value at long times) is plotted for two different photoexcitation energies as a function of the delay time between photoexcitation of mass selected clusters by a nanosecond laser and mass analysis. The experimental time window easily allows the determination of decay rates approximately two orders of magnitude apart. The offset of about 0.5 is due to higher order photoexcitation of the clusters, but does not affect the determination of the decay rates shown since the corresponding decay is typically many orders of magnitude faster. In the case of Fig. 4, absorption of two photons instead of one already leads to a decay roughly eight orders of magnitude faster than the ones shown and can therefore clearly be separated. This is in general valid

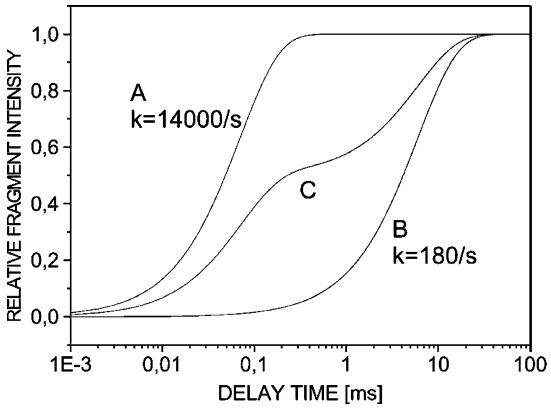

Fig. 5. Expected experimental signature of the product cluster intensity as a function of delay time for three different cases: (A) a hypothetical isomer II with a rate of 14 000 s^{-1}, (B) a hypothetical isomer I with a rate of 180 s^{-1}, (C) an ensemble consisting of equal parts of isomers I and II.

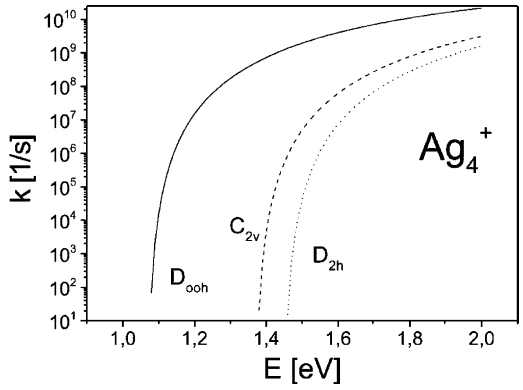

Fig. 6. Rates of fragmentation as a function of the excitation energy for the isomers of Ag_4^+ when dissociation energies of 1.45 eV (D_{2h}), 1.37 eV (C_{2v}) and 1.07 eV ($D_{\infty h}$) [4] are assumed. For the calculation according to Eq. (2) the scaled bulk heat capacities [53] have been used in the parametrization given in [54] with parameters $a = -0.7375$ eV, $b = 10.6$ and $c = 20.9\,\mathrm{eV}^{-1}$. The cross section σ has been assumed geometric, i.e. $\sigma(n) = \pi n^{2/3} r_S^2$ where r_S is the Wigner–Seitz radius of the neutral atom (1.60 Å).

for clusters as small as the present ones and for sufficiently high photon energies as have been used here.

Fig. 5 shows the expected experimental signature of the product cluster intensity as a function of delay time between photoexcitation of mass selected clusters by a nanosecond laser and mass analysis for three different cases: (A) the product cluster intensity of a decay of a hypothetical isomer II with a rate of 14 000 s^{-1}, (B) the same for the decay of an isomer I with a rate of 180 s^{-1} and (C) the product cluster intensity if an ensemble consisting of equal parts of isomers I and II is assumed. Note that for the present purpose of illustrating the effect of the presence of different isomers, it is equivalent to show the time-resolved decay of a single species at different excitation energies and the time-resolved decay of different isomers at a single excitation energy. The line shape of curve C clearly shows a deviation from a single exponential as given by Eq. (3). Instead, it is given by Eq. (4). Obviously, a TRPD experiment as shown in Fig. 4 will reveal the presence of isomers in a given mass-selected ensemble even if the ratio of the decay rates were closer to unity and if the ratio of the isomeric abundances were not as close to unity as assumed in the example of the figure. By the way, this latter ratio would be an experimental result which arises automatically from a respective fit to the data. An estimate of the smallest difference in rate constants which can be observed in a experiment of similar statistics as the ones shown in Fig. 4, gives a factor of about 20. This corresponds to a difference in dissociation energy of about 10%. The use of a trap allows both the zero time and the asymptotic yield to be established with good confidence. This allows a more stringent test for biexponential decay than is possible in experiments where this is not the case.

For large systems such as Au_{38}, Au_{55} and Au_{75}, the difference in binding energy per atom between structures is in general below 10 meV [15] and it can therefore be considered impossible to distinguish between those structures in photodissociation experiments, especially since multi-photon excitation is required for dissociation of these systems on relevant experimental time scales. It can be expected that this holds for elements different from gold, too. If multiphoton-excitation needs to be considered, the assignment of the described experimental signatures is not unambiguous in all cases since the number distribution of absorbed photons is in general unknown. It is therefore in most cases necessary to remain in the single-photon regime. This generally restricts applications to small systems.

For small metal clusters below about $n = 10$ the differences in binding energy between different isomers is typically 0.1 eV, but in some cases like Ag_n, $n = 4$–6, the energy differences even reach values up to about 0.3 eV [4–6,10,16–18].

As a further numerical example in a case where isomers are expected, Fig. 6 shows the calculated decay rates as a function of excitation energy for the three isomers of Ag_4^+. The respective dissociation energies have been reported to be 1.45 eV (D_{2h}), 1.37 eV (C_{2v}) and 1.07 eV ($D_{\infty h}$) [4]. This seems to be an ideal case: at the proper choice of the excitation energy, which is accessible by single-photon absorption, the decay rates are several orders of magnitude apart and in the typical experimental time window.

In such favorable cases, the proposed method may even be used for isomer selection, i.e. for production of ion ensembles which consist of one isomer, only. When the differences in energies are known from systematic scanning, the most stable isomer can be selected by photofragmentation of all other isomers of the ensemble and subsequent isolation, e.g. in trap experiments by mass-selected ejection of all fragment ions. Both pulsed photoexcitation and cw-laser irradiation may be applied if the most stable isomer is cooled non-destructively (e.g. radiatively or by collisions) sufficiently fast enough to avoid an accumulating photoexcitation. This application is of course by design limited to the most stable isomer.

4.2. Constraints on initial energy distribution

With the introduction of the microcanonical temperature it is also possible to estimate the permissible width of the energy distribution that still allows to experimentally observe different decay rates for the isomers. The two apparent rate constants become indistinguishable when $D_I/T_I = D_{II}/T_{II}$, which, with $T_{II} = T_I + \delta T$ translates to

$$\delta T < T_I \frac{\Delta D}{\bar{D}} \rightarrow \delta E < cT \frac{\Delta D}{\bar{D}} \quad (5)$$

The width of the energy distributions of the clusters is mainly the width of the distributions from the source or after a later equilibration to a known temperature. The latter is the case, e.g. the experiments with trapped particles described in [43], where the particles were equilibrated by a gas pulse to ambient temperature. The width of the photon excitation energy is negligible when the number of absorbed photons is small enough for an experimental determination. Also the radiative cooling can induce a width in the energy distribution. For small clusters this is expected to be negligible, because the emission of a single photon tends to quench the unimolecular decay, or at least to change the rate constant so much that the cooled cluster is effectively removed from the observed distribution [54].

Under these assumptions, Eq. (5) and the width of the thermal distribution of $\delta E_{th} = T_{th}\sqrt{c_{th}}$ [56] gives the following constraint:

$$T_{th}\sqrt{c_{th}} < cT \frac{\Delta D}{\bar{D}} \quad (6)$$

For the example of gold clusters Au_5^+, Au_8^+ and Au_{12}^+ as given in Fig. 3, the permissible temperatures $T_{th,max}$ of the initial distribution are 390, 300 and 250 K, respectively, if isomers with a difference in dissociation energy of 0.1 eV are to be distinguished at decay rates of about $1000\,s^{-1}$. For the case of Ag_4^+, the permissible temperature is as high as 1750 K for the distinction of the isomers $D_{\infty h}$ ($D = 1.07$ eV) and C_{2v} ($D = 1.37$ eV) due to the high energy difference and the small size of the system.

5. Conclusion

For sufficiently small systems and dissociation energies within the reach of single-photon excitation, isomeric structures can be distinguished in dedicated time-resolved photodissociation experiments by their difference in decay rates. In particular, small monovalent metal clusters like Ag_4^+ appear to be good candidates for the application of such an approach. In addition, the most stable isomer may be selected from a mass-selected ensemble by photodissociation of all less stable isomers.

Acknowledgements

This work was funded by the Deutsche Forschungsgemeinschaft and the EU network "CLUSTER COOLING."

References

[1] K. Fauth, U. Kreibig, G. Schmidt, Z. Phys. D 12 (1989) 515.
[2] H. Feld, et al., Z. Phys. D 17 (1990) 73.
[3] M. Hermann, U. Kreibig, G. Schmidt, Z. Phys. D 26 (1993) 1.
[4] V. Bonačić-Koutecký, et al., J. Chem. Phys. 98 (1993) 7981.
[5] V. Bonačić-Koutecký, et al., Z. Phys. D 26 (1993) 287.
[6] V. Bonačić-Koutecký, P. Fantucci, J. Koutecký, in: H. Haberland (Ed.), Clusters of Atoms and Molecules, Berlin, 1994, p. 15.
[7] D.J. Wales, J.P.K. Doye, J. Chem. Phys. 103 (1995) 3061.
[8] J.P.K. Doye, D.J. Wales, Science 271 (1996) 484.
[9] J.P.K. Doye, D.J. Wales, Z. Phys. D 40 (1997) 466.
[10] R. Poteau, et al., Z. Phys. D 40 (1997) 479.
[11] C.L. Cleveland, et al., Z. Phys. D 40 (1997) 503.
[12] S. Kümmel, M. Brack, P.G. Reinhard, Phys. Rev. B 58 (1998) 1774.
[13] I.L. Garzon, et al., Eur. Phys. J. D 9 (1999) 211.
[14] F. Baletto, et al., Phys. Rev. Lett. 84 (2000) 5544.
[15] I.L. Garzon, et al., Phys. Rev. Lett. 81 (2000) 1600.
[16] H. Grönbeck, W. Andreoni, J. Chem. Phys. 262 (2000) 1.
[17] H. Häkkinen, U. Landman, Phys. Rev. B 62 (2000) R2287.
[18] R. Fournier, J. Chem. Phys. 115 (2001) 2165.
[19] H.J. Eisler, et al., J. Phys. Chem. A 102 (1998) 3889.
[20] M. Knupfer, et al., Chem. Phys. Lett. 258 (1996) 513.
[21] M. Benz, et al., J. Phys. Chem. 100 (1996) 13399.
[22] P. Weis, J. Chem. Phys. 117 (2002) 9293.
[23] D.E. Clemmer, M.F. Jarrold, J. Mass Spectrom. 32 (1997) 577.
[24] F. Furche, et al., J. Chem. Phys. 117 (2002) 6982.
[25] P. Weis, et al., Chem. Phys. Lett. 355 (2002) 355.
[26] S. Gilb, J. Chem. Phys. 116 (2002) 4094.
[27] R. Fromherz, G. Ganteför, A. Shvartsburg, Phys. Rev. Lett. 89 (2002) 083001.
[28] J. Oviedo, R.E. Palmer, J. Chem. Phys. 117 (2002) 9548.
[29] S. Krückeberg, et al., Phys. Rev. Lett. 85 (2000) 4494.
[30] V. Weisskopf, Phys. Rev. 52 (1937) 259.
[31] P.C. Engelking, J. Chem. Phys. 87 (1987) 936.
[32] P. Fröbich, Phys. Lett. A 202 (1995) 99.
[33] S. Frauendorf, Z. Phys. D 35 (1995) 191.
[34] K. Hansen, Philos. Mag. B 79 (1999) 1413.
[35] R.C. Dunbar, Int. J. Mass Spectrom. 200 (2000) 571.
[36] R.C. Dunbar, in: P.B. Armentrout (Ed.), The Encyclopedia of Mass Spectrometry, vol. 1 (Theory and Ion Chemistry), Elsevier, Amsterdam, 2003, p. 403.
[37] U. Ray, M.F. Jarrold, J.E. Bower, J.S. Kraus, J. Chem. Phys. 91 (1989) 2912.
[38] C. Walther, et al., Chem. Phys. Lett. 256 (1995) 77.
[39] C. Walther, et al., Z. Phys. D 38 (1996) 51.
[40] Y. Shi, V.A. Spasov, K.M. Ervin, J. Chem. Phys. 111 (1999) 938.
[41] V.A. Spasov, Y. Shi, K.M. Ervin, Chem. Phys. 262 (2000) 75.
[42] U. Hild, et al., Phys. Rev. A 57 (1998) 2786.
[43] M. Vogel, K. Hansen, A. Herlert, L. Schweikhard, Phys. Rev. Lett. 87 (2001) 013401.
[44] M. Vogel, K. Hansen, A. Herlert, L. Schweikhard, J. Phys. B 36 (2003) 1073.
[45] C. Bréchignac, et al., J. Chem. Phys. 101 (1994) 6992.
[46] S. Krückeberg, Int. J. Mass Spectrom. Ion Proc. 155 (1996) 141.
[47] O. Ingolfsson, et al., J. Chem. Phys. 112 (2000) 4613, 1713.
[48] V.A. Spasov, et al., Chem. Phys. 262 (2000) 75.

[49] S. Krückeberg, et al., J. Chem. Phys. 114 (2001) 2955.
[50] M. Vogel, K. Hansen, A. Herlert, L. Schweikhard, Eur. Phys. J. D 16 (2001) 73.
[51] K. Hansen, et al., Phys. Rev. Lett. 87 (2001) 123401.
[52] M. Vogel, et al., in preparation.
[53] D.R. Lide (Ed.), CRC Handbook, 78th ed., Boca Raton, 1998.
[54] C. Walther, et al., Phys. Rev. Lett. 83 (1999) 3816.
[55] L. Schweikhard, et al., Eur. Phys. J. D 9 (1999) 15.
[56] R. Balian, From Microphysics to Macrophysics, Springer, Berlin, 1991.